

# Characterizing First Arrival Position Channels: Noise Distribution and Capacity Analysis

Yen-Chi Lee, Yun-Feng Lo, Jen-Ming Wu, *Member, IEEE*,  
and Min-Hsiu Hsieh, *Senior Member, IEEE*

## Abstract

This paper addresses two fundamental problems in diffusive molecular communication: characterizing the first arrival position (FAP) density and bounding the information transmission capacity of FAP channels. Previous studies on FAP channel models, mostly captured by the density function of noise, have been limited to specific spatial dimensions, drift directions, and receiver geometries. In response, we propose a unified solution for identifying the FAP density in molecular communication systems with fully-absorbing receivers. Leveraging stochastic analysis tools, we derive a concise expression with universal applicability, covering any spatial dimension, drift direction, and receiver shape. We demonstrate that several existing FAP density formulas are special cases of this innovative expression. Concurrently, we establish explicit upper and lower bounds on the capacity of three-dimensional, vertically-drifted FAP channels, drawing inspiration from vector Gaussian interference channels. In the course of deriving these bounds, we unravel an explicit analytical expression for the characteristic function of vertically-drifted FAP noise distributions, providing a more compact characterization compared to the density function.

This paper was submitted in part to 2023 IEEE Global Communications Conference (IEEE GLOBECOM), Kuala Lumpur, Malaysia. The two preprints are listed in References as [1], [2].

Yen-Chi Lee, Jen-Ming Wu and Min-Hsiu Hsieh are all affiliated with Hon Hai (Foxconn) Research Institute, Taipei, Taiwan. Emails: yenchilee1925@gmail.com, jen-ming.wu@foxconn.com, min-hsiu.hsieh@foxconn.com

Yun-Feng Lo is affiliated with Georgia Institute of Technology, Atlanta, Georgia, United States. Email: ylo49@gatech.edu

Notably, this expression sheds light on a previously undiscovered weak stability property intrinsic to vertically-drifted FAP noise distributions.

### Index Terms

molecular communication, first arrival position density, capacity bounds, covariance constraint

## I. INTRODUCTION

The challenge of transmitting information over long distances while maintaining the fidelity of the information has been present throughout human history, from ancient times to the present day. While modern communication systems have addressed this problem using electromagnetic signals, such techniques encounter limitations in nano-scale applications due to restrictions in wavelength, antenna size, and energy requirements [3], [4]. To circumvent these restrictions, molecular signals have been proposed as a viable alternative, particularly for nanonetwork applications [5], [6].

In molecular communication (MC) systems, information is conveyed through tiny molecules, referred to as message molecules (MMs), that act as information carriers [7]. To transport these MMs through the physical channel toward a receiver, a propagation mechanism is necessary. Various forms of propagation mechanisms exist, such as diffusion-based [8], flow-based [9], or an engineered transport system like molecular motors [10]. Of these, diffusion-based propagation, often combined with advection (or chemical reaction networks [11]), has been the prevalent approach considered in the literature thus far. In this study, we will focus on *diffusion-based* (also known as *diffusive*) MC systems. Note that we use the terms “molecules” and “particles” interchangeably to refer to the MMs, as their shape is not relevant to our discussion.

In diffusive MC systems, information can be transmitted by modulating various physical properties of the MMs [12]. Once these signaling molecules reach the vicinity of the receiver, they can be detected and processed to extract the required information for detection and decoding

[13]. The reception mechanism of an MC receiver can be classified into two categories: i) passive reception, and ii) active reception [14]. A simple active reception model is the fully-absorbing receiver [15], capable of measuring the hitting time or position of each MM and promptly removing the MM upon reception [16]. In this study, we will focus on fully-absorbing receivers, abbreviated as absorbing receivers for short.

Absorbing receivers harness the information extracted during the initial contact between MMs and the receiver boundary. In this paper, we categorize the modulation schemes applicable to absorbing receivers into three types: timing-based [17], position-based [18], [19], and joint timing-position-based schemes [16]. Numerous studies within the MC field have explored channel properties for timing-based channels [17], [20], [21], whereas investigations into position-based channels are comparatively sparse.

The first part of this paper is dedicated to characterizing first arrival position (FAP) channels, which is formally defined in Section II-B. Prior works, such as [22], have employed a type of stochastic process, known as the first-passage process, to ascertain the FAP density for 3D spherical receivers. Alternatively, [19] examined the FAP density for 2D linear receivers using the image method, a technique reminiscent of electric potential theory [23]. In contrast, we propose an innovative approach to solve the FAP density characterization problem, applicable across various receiver shapes and dimensions. Specifically, we derive a succinct relation

$$f_{\mathbf{Y}|\mathbf{X}}(\mathbf{y}|\mathbf{x}) = \left| \frac{\partial G(\mathbf{x}, \mathbf{y})}{\partial \mathbf{n}_{\mathbf{y}}} \right| \bigg|_{\partial\Omega} \quad (1)$$

which unifies the FAP density calculating problem in different scenarios.

The second part of this paper focuses on exploring the capacity of FAP channels. While the channel capacity of timing-based channels, specifically the AIGN channels, has been extensively studied in the literature [17], [20], [24], [25], the capacity of position-based channels, such as FAP channels, remains elusive. Only a specific case has been discussed, primarily through numerical simulation, in [19, Section IV-B]. In that paper, the authors assume equally spaced

$M$ -ary modulation and employ discretized transition probabilities. Our study aims to fill this gap in the literature by providing analytic capacity bounds for FAP channels without assuming any specific modulation. We study the capacity of additive vertically-drifted (VD) FAP channels

$$C = \sup_{f(\mathbf{X}_{\text{in}}): \mathbb{E}[\mathbf{X}_{\text{in}}\mathbf{X}_{\text{in}}^T] \preceq \Sigma} I(\mathbf{X}_{\text{in}}; \mathbf{X}_{\text{out}}), \quad (2)$$

as detailed in Section V. The supremum is taken over all input distributions  $f(\mathbf{X}_{\text{in}})$  satisfying a *covariance constraint* [26] expressed as  $\mathbb{E}[\mathbf{X}_{\text{in}}\mathbf{X}_{\text{in}}^T] \preceq \Sigma$ , where  $\Sigma \succ 0$ .<sup>1</sup>

The central contributions of this paper encompass a diverse yet interconnected array of aspects. We introduce a novel unified framework capable of calculating the FAP density in diffusive MC systems, applicable to any spatial dimension, drift direction or receiver shape. This provides a comprehensive solution to the FAP density calculating problem for MC systems that deploy fully-absorbing receivers. Notably, our framework goes beyond merely recovering known results on FAP density formulas (see [18], [19]) by generalizing the existing formula for the 2D linear receiver to accommodate arbitrary drift directions (see Appendix A). On the other hand, this paper explores the capacity of FAP channels under a covariance constraint, deriving and proving explicit expressions for both the upper and lower bounds on this capacity for the vertically-drifted case in 3D space. Furthermore, we unravel an explicit analytical expression for the characteristic function of vertically-drifted FAP noise distributions, offering a more succinct characterization compared to the density function. Last but not least, this expression illuminates a hitherto undiscovered weak stability property intrinsic to vertically-drifted FAP noise distributions.

The remainder of this paper is structured as follows. In Section II, we present the physical model and system assumptions used in our analysis. Section III introduces our novel unified approach for finding FAP density. In Section IV, we examine the characteristic function of the VDFAP noise distribution, as well as its weak stability property. We then use the derived

<sup>1</sup>We define the notation  $A \succeq B$  as  $A - B$  being symmetric and positive semi-definite, and  $A \succ B$  as  $A - B$  being symmetric and positive definite. We define  $A \preceq B$  if and only if  $-A \succeq -B$ , and  $A \prec B$  if and only if  $-A \succ -B$ .

formulas for moments and the weak stability property to establish lower and upper bounds for the capacity of VDFAP channels in Section V. Finally, we summarize our results and provide concluding remarks in Section VI.

## II. SYSTEM MODEL

### A. Physical Model

There are two different perspectives for modeling diffusion phenomenon in molecular communication systems. The macroscopic viewpoint utilizes the diffusion equation, also known as the heat equation (both are partial differential equation (PDE) models), to depict the evolution of the concentration  $c(\mathbf{x}, t)$  of message molecules. Based on Fick's law of diffusion [13], the temporal evolution of  $c(\mathbf{x}, t)$ , assuming no chemical reactions, can be described as [13, eq. (17)]:

$$\partial_t c(\mathbf{x}, t; \mathbf{x}_0) + \nabla \cdot (\mathbf{v}(\mathbf{x}, t) c(\mathbf{x}, t; \mathbf{x}_0)) = D \Delta c(\mathbf{x}, t; \mathbf{x}_0), \quad (3)$$

where  $\mathbf{x}_0$  denotes the emission point,  $\mathbf{v}$  denotes the background velocity field,  $\nabla \cdot$  represents the divergence operator, and  $\Delta$  is the Laplacian operator [27]. Here,  $D$  is the diffusion coefficient [13], which we assume to be constant with respect to space and time. The value of  $D$  is dependent on factors such as temperature, fluid viscosity, and the molecule's Stokes radius, as outlined in [7]. Note that the shorthand notations  $\partial_t$  stands for  $\frac{\partial}{\partial t}$  and  $\partial_{x_j}$  stands for  $\frac{\partial}{\partial x_j}$ .

In contrast, from a microscopic perspective, a suitable model for an individual trajectory  $\mathbf{X}_t$  of a message molecule is an Itô diffusion process [28]. We will assume that the parameters in the diffusion channel vary slowly over time, allowing the MC channel to be viewed as an approximately time-invariant system [13]. This assumption corresponds to the time-homogeneous Itô diffusion model. Namely, a *time-homogeneous Itô diffusion* process is a stochastic process that satisfies a stochastic differential equation (SDE) of the form [29, Section 6.2.1]:

$$d\mathbf{X}_t = \mathbf{b}(\mathbf{X}_t) dt + \sigma(\mathbf{X}_t) d\mathbf{B}_t, \quad (4)$$

where  $\mathbf{B}_t$  is a  $D$ -dimensional standard Brownian motion. The first term,  $\mathbf{b}(\mathbf{X}_t) dt$ , is the deterministic component, which describes the drift effect induced by an external potential field. The second term,  $\sigma(\mathbf{X}_t) d\mathbf{B}_t$ , represents the random fluctuations caused by the constant bombardment of background molecules. Notice that  $\mathbf{b}(\cdot)$  is a  $D$ -dimensional vector, and  $\sigma(\cdot)$  is a  $D \times D$  matrix. Both are functions of the spatial variable  $\mathbf{x}$ .

These two models, PDE and SDE, possess an important relation. The microscopic perspective via the SDE (4) can be connected to the macroscopic perspective via the PDE (3) through the Fokker-Planck equation, also known as the Kolmogorov forward equation [28]. Specifically, for an Itô diffusion process  $\mathbf{X}_t$  satisfying (4) for  $t > 0$  and the initial condition  $\mathbf{X}_0 = \mathbf{x}_0$ , the probability density of  $\mathbf{X}_t$ , denoted by  $p(\mathbf{x}, t; \mathbf{x}_0)$ , satisfies the Kolmogorov forward equation:

$$\partial_t p(\mathbf{x}, t; \mathbf{x}_0) = - \sum_{j=1}^D \partial_{x_j} [b_j(\mathbf{x}) p(\mathbf{x}, t; \mathbf{x}_0)] + \sum_{j=1}^D \sum_{k=1}^D \partial_{x_j} \partial_{x_k} [D_{jk}(\mathbf{x}) p(\mathbf{x}, t; \mathbf{x}_0)] \quad (5)$$

where  $b_j(\mathbf{x})$  denotes the  $j$ -th component of  $\mathbf{b}(\mathbf{x})$  and  $D_{jk}(\mathbf{x})$  is the  $(j, k)$ -th entry of the matrix  $D(\mathbf{x}) := \frac{1}{2} \sigma(\mathbf{x}) \sigma(\mathbf{x})^\top$ . To establish a connection between (5) and (3), we make two assumptions that are common in the MC literature [7], [13]: i) the background velocity field is constant with respect to time, i.e., assuming  $\mathbf{v}(\mathbf{x}, t) = \mathbf{v}(\mathbf{x})$  in the macroscopic PDE model; ii) the diffusion coefficient  $D$  is constant throughout space and time. That is, we assume the matrix  $\sigma(\mathbf{x})$  to be a scalar multiple of the identity matrix, where the scalar is a constant. To simplify notations, we also denote this scalar constant by  $\sigma$ . Under these two assumptions, we can establish equivalence between (3) and (5) by identifying the following quantities:  $c = p$ ,  $\mathbf{v}(\cdot) = \mathbf{b}(\cdot)$  and  $D = \sigma^2/2$ .<sup>2</sup>

### B. Communication Model

In this paper, we investigate a diffusive molecular communication system, which employs the emission positions of MMs in a  $D$ -dimensional fluid medium to convey information. In

<sup>2</sup>Note that since (3) and (5) are *linear* PDEs, any scalar multiple of a solution is still a solution. In concentration-encoded MC where MMs move independently, the relation  $c = N_{\text{total}} \cdot p$  holds ( $N_{\text{total}}$  denotes the total number of MMs released) [13].

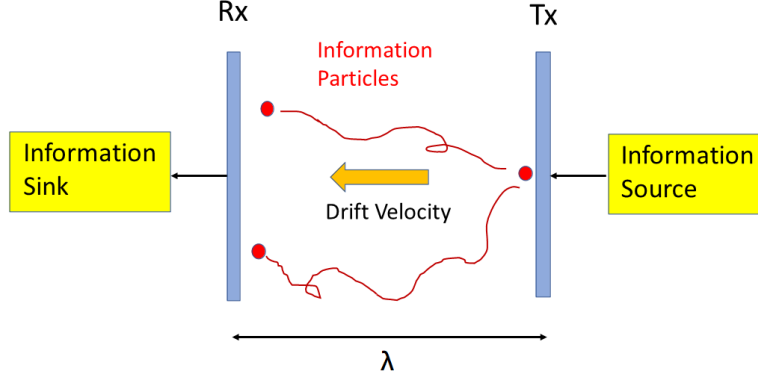


Fig. 1. This figure illustrates a 2D FAP channel with line-shape Tx and Rx, where the Tx is assumed to be transparent, allowing particles to move through it without experiencing any force. The emission point is located on the line-shape Tx.

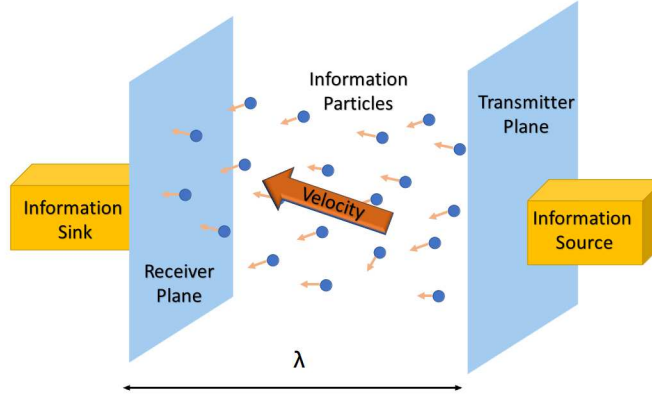


Fig. 2. This figure illustrates a 3D FAP channel with plane-shape Tx and Rx, where the Tx is assumed to be transparent, allowing particles to move through it without experiencing any force. The emission point is located on the Tx plane.

practice,  $D = 2, 3$  are commonly selected. See Fig. 1 and Fig. 2. We consider a scenario where there is a constant velocity field [9] in the ambient space. This corresponds to further assuming  $\mathbf{v}(\cdot) = \mathbf{b}(\cdot) = \mathbf{v}$ , where  $\mathbf{v}$  is a constant vector. We call  $\mathbf{v}$  the drift (vector) hereafter. Additionally, we assume all the MMs are of the same type [30]. The diffusion effects of MMs are captured by a diffusion coefficient  $D = \sigma^2/2$ , which is assumed to be a constant throughout space and time [7]. We call this the isotropic assumption on the fluid medium.

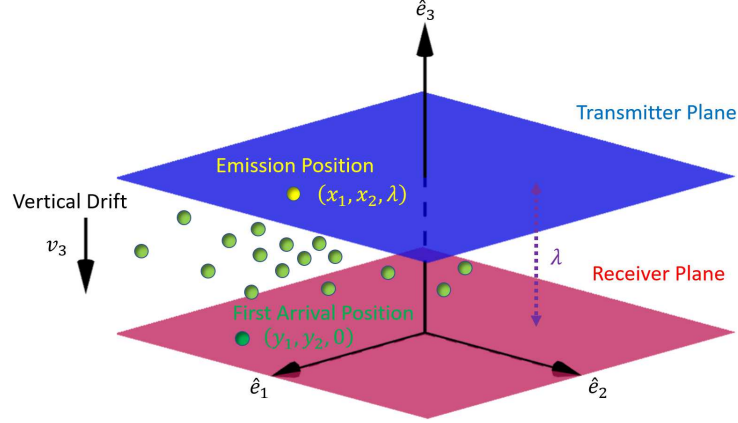


Fig. 3. This figure is a conceptual diagram of a 3D MC system where both the Tx and Rx have plane shapes. The communication takes place in a fluid medium with a vertical drift  $v_3 < 0$ , and the transmission distance is denoted by  $\lambda > 0$ . The orthonormal basis vectors for this 3D space are denoted by  $\{\hat{e}_i\}_{i=1}^3$ , and the *position information* is embedded in the first two coordinates.

The MC system we considered comprises a transmitter (Tx) and a receiver (Rx), which are modeled as parallel D-dimensional hyperplanes (hereafter referred to as *planes*) separated by a distance  $\lambda > 0$ . Without loss of generality, we can set the Tx plane at coordinate  $x_D = \lambda$  and the Rx plane at coordinate  $x_D = 0$ . Fig. 3 demonstrates the 3D case with a vertical drift.

In this study, we assume an ideal MC system that satisfies the following assumptions:

- (A1) The transmitter has perfect control over the emission position of the MMs.
- (A2) The transmitter plane is transparent, allowing MMs to move through it without experiencing any force after they are released.
- (A3) The receiver can perfectly measure the first arrival positions of the MMs.
- (A4) Upon first arrival at the receiver plane, MMs are captured and removed from the system.
- (A5) The movement of every MM is independent.

Although the ambient space is D-dimensional, the position information is  $d$ -dimensional, where  $d := D - 1$  for brevity and consistency throughout this paper. The first arrival position  $\mathbf{Y}$  of a



molecule released at position  $\mathbf{X}$  can be expressed as

$$\mathbf{Y} = \mathbf{X} + \mathbf{N}, \quad (6)$$

where  $\mathbf{N}$  denotes the deviation (i.e., noise) of the first arrival position. The probability density function of  $\mathbf{N}$  is defined to be the *FAP density* [18], [19], and the additive channel (6) is defined to be the *FAP channel*.

In order to express the FAP density formula presented in the next subsection, we write the D-dimensional drift vector  $\mathbf{v} = [v_1, \dots, v_D]^\top$  as  $\mathbf{v} = [\mathbf{v}_{\text{par}}, v_D]^\top$ , where  $\mathbf{v}_{\text{par}} := [v_1, \dots, v_d]^\top$  contains the drift components parallel to the Tx and Rx planes, and  $v_D$  is the drift component perpendicular to the Tx and Rx planes. As a rule of thumb, we use **bold fonts** to stand for (column) vectors; slanted **vectors** are  $d$ -dimensional, while non-slanted **vectors** are D-dimensional. The operator  $(\cdot)^\top$  represents transposition. We also introduce the notation  $\mathbf{u} := \frac{\mathbf{v}}{\sigma^2}$  and similarly for  $\mathbf{u}_{\text{par}}$  and  $u_1, \dots, u_D$ . These  $\{u_j\}_{j=1}^D$  can be interpreted as normalized drift.

### C. The FAP Noise Distribution

In [18], [19], the 2D and 3D FAP densities were separately derived based on different methods. By the framework proposed in this paper, we can unify the derivations in different scenarios into a standard procedure. Our new derivation, which recovers the FAP formulas in [18], [19], is presented in Appendix A. Notice that the special function  $K_{\frac{3}{2}}$  has an elementary form [31]:

$$K_{\frac{3}{2}}(x) = \sqrt{\frac{\pi}{2}} e^{-x} \left( \frac{1+x}{x^{\frac{3}{2}}} \right), \quad (7)$$

where  $K_\nu(\cdot)$  denotes the order- $\nu$  modified Bessel function of the second kind [27]. Substituting (7) into the formula (67) for the 3D planar receiver case and denoting  $\mathbf{n} = \mathbf{y} - \mathbf{x}$ , we can merge the two FAP densities, for  $D = 2$  (62) and  $D = 3$  (67), into a single expression:

$$f_{\mathbf{N}}^{(d)}(\mathbf{n}; \mathbf{u}, \lambda) = 2\lambda \frac{\|\mathbf{u}\|^{\frac{d+1}{2}}}{(2\pi)^{\frac{d+1}{2}}} \cdot e^{\mathbf{u}_{\text{par}}^\top \mathbf{n} - u_D \lambda} \cdot \frac{K_{\frac{d+1}{2}} \left( \|\mathbf{u}\| \sqrt{\|\mathbf{n}\|^2 + \lambda^2} \right)}{\left( \sqrt{\|\mathbf{n}\|^2 + \lambda^2} \right)^{\frac{d+1}{2}}}, \text{ for } \mathbf{n} \in \mathbb{R}^d, \quad (8)$$

where  $\|\cdot\|$  denotes the Euclidean norm.

For the channel capacity investigation, we focus on a sub-family of FAP (noise) distributions with two specific properties:

- i) The parallel drift components are zero, i.e.,  $\mathbf{v}_{\text{par}} = \mathbf{0}$ .
- ii) The *vertical drift* (VD) component points from the Tx to the Rx, i.e.,  $v_D < 0$ . (Intuitively, this vertical drift helps the transmission of information.)

We name this sub-family as vertically-drifted first arrival position (VDFAP) distributions because only the vertical drift component is non-zero. We can set  $\mathbf{u}_{\text{par}} = \mathbf{0}$  so that  $\|\mathbf{u}\|$  in (8) becomes  $|u_D| = -u_D$ . Abbreviating  $u_D$  as  $u$ , the VDFAP densities can be expressed as:

$$f_{\mathbf{N}}^{(d)}(\mathbf{n}; u, \lambda) = 2\lambda \left( \frac{|u|}{\sqrt{2\pi}} \right)^{d+1} \cdot e^{\lambda|u|} \cdot \frac{K_{\frac{d+1}{2}} \left( |u| \sqrt{\|\mathbf{n}\|^2 + \lambda^2} \right)}{\left( |u| \sqrt{\|\mathbf{n}\|^2 + \lambda^2} \right)^{\frac{d+1}{2}}}, \text{ for } \mathbf{n} \in \mathbb{R}^d. \quad (9)$$

We also denote the VDFAP densities by  $f_{\mathbf{N}}^{(d)}(\mathbf{n})$  when the parameters  $u, \lambda$  are clear from the context. As a shorthand, we denote  $\mathbf{N} \sim \text{VDFAP}^{(d)}(u, \lambda)$  if a  $d$ -dimensional random vector  $\mathbf{N}$  follows the VDFAP distribution defined by (9) with parameters  $u < 0$  and  $\lambda > 0$ . Note that we refer to a random variable  $X \in \mathbb{R}$  as a “one-dimensional random vector” to maintain consistency in terminology.

### III. A NOVEL FRAMEWORK FOR EFFICIENTLY DETERMINING FAP DENSITY

In this section, we propose a novel and unified framework for determining the FAP density. To achieve this goal, we introduce several stochastic analytical tools, such as the generator of diffusion semigroup and Dynkin’s formula [29].

Our new method for calculating the FAP density can be divided into three steps as summarized in Table I. Specifically, the FAP density can be computed as  $f_{\mathbf{Y}|\mathbf{X}}(\mathbf{y}|\mathbf{x}) = \left| \frac{\partial G(\mathbf{x}, \mathbf{y})}{\partial \mathbf{n}_{\mathbf{y}}} \right|$  once the elliptic Green’s function  $G(\mathbf{x}, \mathbf{y})$  is known. Note that the “previous method” in Table I refers to those methods that tackle the diffusion equation (3) directly, such as [19].

TABLE I  
COMPARISON BETWEEN PREVIOUS AND NEW METHOD OF CALCULATING FAP DENSITY

	Previous Method	New Method
<b>Step 1</b>	Calculates the free space Green's function for parabolic-type [27] PDE.	Removes time-dependency via considering the generator of the diffusion semigroup.
<b>Step 2</b>	Accommodates the free space solution to absorbing boundary conditions (e.g., using the image method).	Solves elliptic-type [27] boundary value problem with appropriate boundary conditions.
<b>Step 3</b>	Calculates the flux density [19] and does integration with respect to time.	Obtains FAP density directly from the Green's function $G(\mathbf{x}, \mathbf{y})$ . No time-integration is required.

For the previous method, a parabolic-type PDE (which is time-dependent) is used, while the new method removes the time-dependency by considering the generator of the diffusion semigroup. As a consequence, using the previous method often requires doing integration with respect to time, which is unnecessary while applying our new method.

In the remainder of this section, we will establish the validity of the proposed FAP density computing framework.

#### A. Infinitesimal Generator of Itô Diffusion

Recall that a D-dimensional Itô diffusion is a stochastic process that satisfies (4):  $d\mathbf{X}_t = \mathbf{b}(\mathbf{X}_t) dt + \sigma(\mathbf{X}_t) d\mathbf{B}_t$ . In this subsection, we will first assume that  $\mathbf{b}(\cdot)$  and  $\sigma(\cdot)$  are constant only with respect to time, but not to space, allowing the corresponding channel to be regarded as a time-invariant system. We will make further assumptions on  $\sigma(\cdot)$  as the deductions progress. Nevertheless, for the purpose to calculate FAP density in specific scenarios (as shown in Appendix A), we only need the stronger assumptions as stated in Section II.

For each Itô diffusion  $\mathbf{X}_t$ , a corresponding operator called the infinitesimal generator, or simply generator, can be associated. Let  $\mathcal{D}(A)$  denote the domain of the generator  $A$  [32]. We define

the notation  $\mathbb{E}^{\mathbf{x}}[\cdot]$  as taking expectation conditioned on  $\mathbf{X}_0 = \mathbf{x}$ , so that

$$\mathbb{E}^{\mathbf{x}}[f(\mathbf{X}_t)] := \mathbb{E}[f(\mathbf{X}_t) | X_0 = \mathbf{x}]. \quad (10)$$

The generator  $A$  (which operates on function  $f$ ) of a process  $\mathbf{X}_t$  can be defined as

$$Af = A\{f(\mathbf{x})\} := \lim_{t \searrow 0} \frac{\mathbb{E}^{\mathbf{x}}[f(\mathbf{X}_t)] - f(\mathbf{x})}{t} \text{ for any } f \in \mathcal{D}(A). \quad (11)$$

For time-homogeneous Itô processes  $\mathbf{X}_t$ , the time evolution is a Markov process. By letting  $T_t f := \mathbb{E}^{\mathbf{x}}[f(\mathbf{X}_t)]$ , we can obtain a semigroup of operators  $\mathcal{T} = \{T_t\}_{t \geq 0}$ . Notice that the term

$$Af = \lim_{t \searrow 0} \frac{T_t f - f}{t} \quad (12)$$

can be interpreted as the rate of linear increment with respect to  $t$  through the semigroup evolution.

To explicitly calculate the generator  $A$  based on (4), we can assume that  $f$  is of class  $C^2$ , which means that it has both a continuous first derivative and a continuous second derivative. Using Taylor expansion [29, Formula (9.2.2)] and Itô's formula [28], we have:

$$\begin{aligned} d f(\mathbf{X}_t) &= (\nabla f)^{\top} (d\mathbf{X}_t) + \frac{1}{2} (d\mathbf{X}_t)^{\top} \text{Hess}(f) (d\mathbf{X}_t) \\ &= \left[ (\nabla f)^{\top} (\mathbf{b}(\mathbf{X}_t)) + \text{tr} \left( \text{Hess}(f) \frac{\sigma \sigma^{\top}(\mathbf{X}_t)}{2} \right) \right] dt + (\nabla f)^{\top} \sigma(\mathbf{X}_t) d\mathbf{B}_t, \end{aligned} \quad (13)$$

where  $\text{tr}(\cdot)$  denotes the trace operation,  $\text{Hess}(f)$  denotes the Hessian of  $f$  and the matrix notation  $\sigma \sigma^{\top}(\mathbf{X}_t)$  is short for  $\sigma(\mathbf{X}_t) (\sigma(\mathbf{X}_t))^{\top}$ . Note that in (13), all the gradient  $\nabla f$  and Hessian  $\text{Hess}(f)$  terms are evaluated at  $\mathbf{X}_t$ . After taking expectation to both sides of (13), and then plugging into (11), we use the fact that  $\mathbb{E}[d\mathbf{B}_t] = 0$  to obtain an explicit expression for the generator  $A$  as:

$$A\{f(\mathbf{x})\} = \mathbf{b}(\mathbf{x})^{\top} (\nabla f(\mathbf{x})) + \frac{\sigma^2(\mathbf{x})}{2} \Delta f(\mathbf{x}), \quad (14)$$

where  $\mathbf{x}$  can be viewed as the starting point of a diffusion process. From (14), we can see that  $A$  is a second-order differential operator of elliptic-type. Notice that in (14) we have assumed that the matrix  $\sigma(\cdot)$  is a scalar multiple of the identity matrix. To simplify the notation, we also denoted this scalar function by  $\sigma(\cdot)$  in (14).

We proceed to consider a boundary value problem (BVP) with an unknown function  $\phi \in C^2$ , given by:

$$\begin{cases} A\phi = 0 & \text{in } \Omega \\ \phi = g & \text{on } \partial\Omega \end{cases}, \quad (15)$$

where  $\Omega$  is the domain in which the MMs can diffuse, and  $\partial\Omega$  is the boundary of the domain. In (15),  $A$  denotes a partial differential operator and  $g$  is the prescribed boundary data, which is also a  $C^2$  function. Note that for elliptic-type partial differential operators, representation formulas for commonly encountered boundary conditions can be directly found in PDE handbooks such as [33].

### B. A Novel Relation Between FAP Density and Elliptic Green's Function

Recall the infinitesimal generator defined in (11). By rearranging the terms in (11), we can obtain the following integral expression:

$$\mathbb{E}^{\mathbf{x}} [f(\mathbf{X}_t)] = f(\mathbf{x}) + \mathbb{E}^{\mathbf{x}} \left[ \int_0^t A\{f(\mathbf{X}_s)\} \, ds \right]. \quad (16)$$

It is important to note that the variable  $t$  appearing in (16) is deterministic, not a random variable.

In the field of stochastic analysis, Dynkin's formula relates the expected value of a function  $f$  of a Markov process at a stopping time  $\tau$  [34, Definition 8.2.1] to the initial value  $f(\mathbf{x})$  of the function and an integral involving the generator  $A$  of the process. Technically, we have to make some assumptions on  $f$ . As we are considering a second-order differential operator (14), it is common to require  $f$  to be twice continuously differentiable (i.e.,  $f \in C^2$ ). Letting  $\tau$  be a stopping time such that  $\mathbb{E}^{\mathbf{x}}[\tau] < +\infty$ , the Dynkin's formula can be expressed as:

$$\mathbb{E}^{\mathbf{x}} [f(\mathbf{X}_\tau)] = f(\mathbf{x}) + \mathbb{E}^{\mathbf{x}} \left[ \int_0^\tau A\{f(\mathbf{X}_s)\} \, ds \right]. \quad (17)$$

Notably,  $\tau$  in (17) is now a random variable. Additional details regarding this formula can be found in [29, eq. (9.3.10)].

Let  $g$  denote a smooth function defined on the boundary  $\partial\Omega$ . We can express the expected value of  $g(\mathbf{X}_\tau)$  as follows:

$$\mathbb{E}^\mathbf{x}[g(\mathbf{X}_\tau)] = \mathbb{E}\left[g(\mathbf{X}_\tau) \middle| \mathbf{X}_0 = \mathbf{x}\right] = \int_{\partial\Omega} f_{\mathbf{Y}|\mathbf{X}}(\mathbf{y}|\mathbf{x})g(\mathbf{y}) \, dS_{\mathbf{y}}, \quad (18)$$

where  $dS_{\mathbf{y}}$  is the magnitude of surface element at  $\mathbf{y}$  [27]. Here,  $\mathbf{x} \in \Omega$  represents the starting point (corresponding to the emission point) of the diffusion, while the hitting position  $\mathbf{y}$  belongs to the boundary, i.e.,  $\mathbf{y} \in \partial\Omega$ .

The conditional probability density function  $f_{\mathbf{Y}|\mathbf{X}}$  in (18) can be interpreted as the distribution of the position of  $\mathbf{X}_t$  at the stopping time  $\tau$ . In MC applications,  $\mathbf{X}_t$  is the trajectory of a MM, and the stopping event corresponds to the capture by Rx. Thus,  $f_{\mathbf{Y}|\mathbf{X}}$  is the desired FAP density on the receiver boundary  $\partial\Omega$ . Our remaining task is to express  $f_{\mathbf{Y}|\mathbf{X}}$  using the Green's function.

Suppose we have a solution  $\phi(\mathbf{x})$  for the BVP in (15) with prescribed boundary data  $g$  such that  $A\phi = 0$  inside  $\Omega$ . By setting  $f(\mathbf{x}) = \phi(\mathbf{x})$  in (17), we obtain  $\int_0^\tau A\{\phi(\mathbf{X}_s)\} \, ds = 0$ . Here,  $\tau$  represents the first hitting time. The physical interpretation of this condition is that  $\mathbf{X}_s$  is located inside  $\Omega$  prior to the hitting event, which leads to  $A\{\phi(\mathbf{X}_s)\} = 0$  for  $0 < s < \tau$ . Furthermore, since  $\phi(\mathbf{x})$  coincides with  $g(\mathbf{x})$  on the boundary, we can express the left-hand side of (17) as  $\mathbb{E}^\mathbf{x}[g(\mathbf{X}_\tau)]$ . Combining these two facts yields:

$$\mathbb{E}^\mathbf{x}[g(\mathbf{X}_\tau)] = \phi(\mathbf{x}) + 0 = \int_{\partial\Omega} f_{\mathbf{Y}|\mathbf{X}}(\mathbf{y}|\mathbf{x})g(\mathbf{y}) \, dS_{\mathbf{y}}. \quad (19)$$

This holds true for any  $\mathbf{x} \in \Omega$ .

For a general elliptic-type BVP defined in a domain  $\Omega$  with boundary  $\partial\Omega$ , it is true that [33]:

$$u(\mathbf{x}) = \int_{\Omega} \Xi(\mathbf{y})H_1(\mathbf{x}, \mathbf{y}) \, dV_{\mathbf{y}} + \int_{\partial\Omega} g(\mathbf{y})H_2(\mathbf{x}, \mathbf{y}) \, dS_{\mathbf{y}}. \quad (20)$$

Here,  $\Xi$  represents the source term,  $dV_{\mathbf{y}}$  is the volume element [27],  $dS_{\mathbf{y}}$  is the magnitude of surface element, and  $H_1(\mathbf{x}, \mathbf{y})$ ,  $H_2(\mathbf{x}, \mathbf{y})$  depend on the type of boundary conditions under consideration [33]. For MC systems without molecule reproduction or annihilation inside the

channel, we can set  $\Xi(\mathbf{y}) = 0$ , and hence  $H_1(\mathbf{x}, \mathbf{y})$  is irrelevant. Notice that BVP (15) has the Dirichlet-type boundary condition [27, Chapter 13]. According to [33], we have

$$H_2(\mathbf{x}, \mathbf{y}) = -\frac{\partial G(\mathbf{x}, \mathbf{y})}{\partial \mathbf{n}_{\mathbf{y}}} \quad (21)$$

in the solution formula (20), where  $G$  represents the Green's function of BVP (15). The notation  $\frac{\partial}{\partial \mathbf{n}_{\mathbf{y}}}$  means the directional derivative along the outward normal at the point  $\mathbf{y}$  on  $\partial\Omega$ . Letting  $\Xi = 0$  and plugging (21) into (20), we obtain a simpler form:

$$\phi(\mathbf{x}) = \int_{\mathbf{y} \in \partial\Omega} \left| \frac{\partial G(\mathbf{x}, \mathbf{y})}{\partial \mathbf{n}_{\mathbf{y}}} \right| g(\mathbf{y}) \, dS_{\mathbf{y}}. \quad (22)$$

Note that we have added an absolute value since the term  $\left| \frac{\partial G(\mathbf{x}, \mathbf{y})}{\partial \mathbf{n}_{\mathbf{y}}} \right|$  has the physical meaning of conditional probability density, so it must be non-negative. Finally, by comparing (19) and (22), we can establish a fundamental relation between the FAP density and the elliptic-type Green's function:

$$f_{\mathbf{Y}|\mathbf{X}}(\mathbf{y}|\mathbf{x}) = \left| \frac{\partial G(\mathbf{x}, \mathbf{y})}{\partial \mathbf{n}_{\mathbf{y}}} \right| \Big|_{\partial\Omega}, \quad (23)$$

where  $\Big|_{\partial\Omega}$  means  $\mathbf{y}$  is evaluated on  $\partial\Omega$ . Notice that (23) gives a concise relation between the FAP density function and the Green's function. How to explicitly calculate the FAP density using (23) in specific scenarios is demonstrated in Appendix A.

#### IV. THE CHARACTERISTIC FUNCTION OF VDFAP DISTRIBUTION

In order to obtain analytic bounds for the channel capacity, we conduct a comprehensive analysis of the characteristic function of VDFAP distributions. Additionally, we investigate a newly discovered stability property exhibited by VDFAP distributions.

Based on probability theory, distributions can be characterized by its *characteristic function* (CF) [35, Section 3.3]. The CF viewpoint facilitates the computation of moments and the analysis of stability properties for VDFAP distributions.

For a random vector  $\mathbf{N}$  following  $\text{VDFAP}^{(d)}(u, \lambda)$ , we denote its CF as

$$\Phi_{\mathbf{N}}^{(d)}(\boldsymbol{\omega}; u, \lambda) := \mathbb{E}[\exp(i\boldsymbol{\omega}^\top \mathbf{N})], \text{ for } \boldsymbol{\omega} \in \mathbb{R}^d, \quad (24)$$

where  $i$  denotes the imaginary unit. We also denote the CF simply by  $\Phi_{\mathbf{N}}^{(d)}(\boldsymbol{\omega})$  when the context allows for a clear understanding of the parameters  $u, \lambda$ . We have derived a novel closed-form expression for (24) when  $d = 1, 2$ , detailed in [2, Appendix A], as:

$$\Phi_{\mathbf{N}}^{(d)}(\boldsymbol{\omega}; u, \lambda) = \exp\left(-\lambda\left(\sqrt{\|\boldsymbol{\omega}\|^2 + |u|^2} - |u|\right)\right). \quad (25)$$

Note that letting  $|u| \rightarrow 0$  in the CF formula (25) recovers the  $d$ -dimensional Cauchy CF [36]:

$$\lim_{|u| \rightarrow 0} \Phi_{\mathbf{N}}^{(d)}(\boldsymbol{\omega}; u, \lambda) = \exp(-\lambda\|\boldsymbol{\omega}\|). \quad (26)$$

The observation in (26) indicates that as the drift approaches zero, the density of FAP distribution given by (8) reduces to a Cauchy density.

Via the closed-form CF expression (25), we obtain the formulas of the first two moments, as well as a weak stability property of VDFAP distributions.

#### A. Mean Vector and Covariance Matrix

Based on (24), the mean vector of  $\mathbf{N} \sim \text{VDFAP}^{(d)}(u, \lambda)$  can be calculated as

$$\mathbb{E}[\mathbf{N}] = -i\nabla\Phi_{\mathbf{N}}^{(d)}(\boldsymbol{\omega})\Big|_{\boldsymbol{\omega}=\mathbf{0}}, \quad (27)$$

and the correlation matrix of  $\mathbf{N}$  as

$$\mathbb{E}[\mathbf{N}\mathbf{N}^\top] = -\text{Hess}\left(\Phi_{\mathbf{N}}^{(d)}\right)(\boldsymbol{\omega})\Big|_{\boldsymbol{\omega}=\mathbf{0}}. \quad (28)$$

Note that from [37, Corollary 1 and Corollary 2 of Theorem 2.3.1], equalities in (27) and (28) hold if and only if the Hessian of  $\Phi_{\mathbf{N}}^{(d)}$  at  $\boldsymbol{\omega} = \mathbf{0}$  exists as a matrix with all the entries finite. We will show shortly that this is the case for VDFAP distributions.

We first calculate the gradient of the CF:

$$\nabla\Phi_{\mathbf{N}}^{(d)}(\boldsymbol{\omega}) = \frac{-\lambda\Phi_{\mathbf{N}}^{(d)}(\boldsymbol{\omega})}{\sqrt{\|\boldsymbol{\omega}\|^2 + |u|^2}}\boldsymbol{\omega}. \quad (29)$$



Then we can proceed from (29) to calculate the Hessian of the CF:

$$\text{Hess}\left(\Phi_N^{(d)}\right)(\boldsymbol{\omega}) = \frac{-\lambda\Phi_N^{(d)}(\boldsymbol{\omega})}{\sqrt{\|\boldsymbol{\omega}\|^2 + |u|^2}}\mathbb{I}_d + \frac{\lambda\Phi_N^{(d)}(\boldsymbol{\omega})}{(\|\boldsymbol{\omega}\|^2 + |u|^2)^{\frac{3}{2}}} \left(1 + \lambda\sqrt{\|\boldsymbol{\omega}\|^2 + |u|^2}\right) \boldsymbol{\omega}\boldsymbol{\omega}^\top, \quad (30)$$

where  $\mathbb{I}_d$  denotes the  $d \times d$  identity matrix. From (30), we see that at  $\boldsymbol{\omega} = \mathbf{0}$ , the Hessian of the CF indeed exists as a matrix with finite entries:

$$\text{Hess}\left(\Phi_N^{(d)}\right)(\boldsymbol{\omega})\Big|_{\boldsymbol{\omega}=\mathbf{0}} = -\frac{\lambda}{|u|}\mathbb{I}_d. \quad (31)$$

Note that this fact crucially depends on  $|u| > 0$ , which is the case for VDFAP by definition.<sup>3</sup>

From (27) and (29), we can deduce that  $\mathbb{E}[\mathbf{N}] = \mathbf{0}$ . Alternatively, due to the radial symmetry of  $\mathbf{N}$ , we can also deduce that it has zero mean (whenever the mean is well-defined). Due to the mean being zero, the correlation matrix of  $\mathbf{N}$  coincides with the covariance matrix. Hence, from (28) and (31), the covariance matrix of  $\mathbf{N}$  can be expressed as:

$$\mathbb{E}[\mathbf{N}\mathbf{N}^\top] = \frac{\lambda}{|u|}\mathbb{I}_d. \quad (32)$$

It is interesting to note that the variance of each component of a random vector  $\mathbf{N}$  following  $\text{VDFAP}^{(d)}(u, \lambda)$  is  $\frac{\lambda}{|u|}$ . Also, the components of  $\mathbf{N}$  are pairwise uncorrelated, but not independent, as the PDF (9) cannot be decomposed as the product of its marginal PDFs.

### B. A Weak Stability Property

Gaussian distributions, along with Cauchy distributions and Lévy distributions, are known to be examples of *stable* distributions [30]. These distributions possess a specific form of CF [38], which is not satisfied by (25). Therefore, we can conclude that VDFAP distributions are *not* stable. However, despite not being (strictly) stable, VDFAP distributions still exhibit certain “weaker” stability properties.

<sup>3</sup>As a sanity check, when  $u \rightarrow 0$ , VDFAP distributions reduces to (multivariate) Cauchy distributions, which are known to have no well-defined first and second moments.

One such *weak stability property* that will be useful in deriving a lower bound for the capacity of VDFAP channels is the following: if  $\mathbf{N}_1 \sim \text{VDFAP}^{(d)}(u, \lambda_1)$  and  $\mathbf{N}_2 \sim \text{VDFAP}^{(d)}(u, \lambda_2)$  are two independent VDFAP random vectors with the same normalized drift  $u$ , then their sum  $\mathbf{N}_1 + \mathbf{N}_2 \sim \text{VDFAP}^{(d)}(u, \lambda_1 + \lambda_2)$ .

To prove this property, note that  $\mathbf{N}_1$  and  $\mathbf{N}_2$  are independent. Therefore, the CF of their sum is the product of their respective CFs, i.e.,  $\mathbb{E}[\exp(i\boldsymbol{\omega}^\top(\mathbf{N}_1 + \mathbf{N}_2))] = \Phi_{\mathbf{N}_1}^{(d)}(\boldsymbol{\omega}; u, \lambda_1)\Phi_{\mathbf{N}_2}^{(d)}(\boldsymbol{\omega}; u, \lambda_2)$ .

Using the CF formula (25) for  $\mathbf{N}_1$  and  $\mathbf{N}_2$ , we obtain:

$$\begin{aligned} & \mathbb{E}[\exp(i\boldsymbol{\omega}^\top(\mathbf{N}_1 + \mathbf{N}_2))] \\ &= \exp\left(-\lambda_1 \left(\sqrt{\|\boldsymbol{\omega}\|^2 + |u|^2} - |u|\right)\right) \cdot \exp\left(-\lambda_2 \left(\sqrt{\|\boldsymbol{\omega}\|^2 + |u|^2} - |u|\right)\right) \\ &= \exp\left(-(\lambda_1 + \lambda_2) \left(\sqrt{\|\boldsymbol{\omega}\|^2 + |u|^2} - |u|\right)\right). \end{aligned} \quad (33)$$

Since the CF uniquely characterizes the distribution, we can compare this result to the CF formula (25) again to conclude that  $\mathbf{N}_1 + \mathbf{N}_2 \sim \text{VDFAP}^{(d)}(u, \lambda_1 + \lambda_2)$ .

## V. BOUNDS ON THE CAPACITY OF VDFAP CHANNEL

Borrowing the wisdom from vector Gaussian interference channels [26] we investigate the VDFAP channel capacity under the covariance matrix constraint as follows:

$$C = \sup_{f(\mathbf{X}): \mathbb{E}[\mathbf{X}\mathbf{X}^\top] \preceq \Sigma} I(\mathbf{X}; \mathbf{Y}), \quad (34)$$

where the objective function  $I(\mathbf{X}; \mathbf{Y})$  is the *mutual information* [39] between two  $d$ -dim random vectors  $\mathbf{X}$  and  $\mathbf{Y}$ . The supremum is taken over all input distributions satisfying the covariance<sup>4</sup> constraint  $\mathbb{E}[\mathbf{X}\mathbf{X}^\top] \preceq \Sigma$ , where  $\Sigma$  is a prescribed *positive definite* matrix. Note that the VDFAP channel output  $\mathbf{Y}$  equals to  $\mathbf{X} + \mathbf{N}$ , where the noise  $\mathbf{N}$  follows  $\text{VDFAP}^{(d)}(u, \lambda)$  distribution, and is *independent* of the input  $\mathbf{X}$ . The capacity appeared in (34) depends on the dimension  $d$  and the parameter triplet  $(u, \lambda, \Sigma)$ , so we also write it as  $C^{(d)}(u, \lambda, \Sigma)$  to stress these dependencies.

<sup>4</sup>Although  $\mathbb{E}[\mathbf{X}\mathbf{X}^\top]$  is a correlation matrix, in the context of entropic quantities, we can without loss of generality assume that the mean is zero. So we use the terms *correlation* and *covariance* interchangeably hereafter.

Applying the additive channel structure  $\mathbf{Y} = \mathbf{X} + \mathbf{N}$ , equation (34) can be simplified as:

$$C = \sup_{f(\mathbf{X}): \mathbb{E}[\mathbf{X}\mathbf{X}^T] \preceq \Sigma} h(\mathbf{Y}) - h(\mathbf{N}), \quad (35)$$

where  $h(\mathbf{W})$  denotes the differential entropy of a  $d$ -dim random vector  $\mathbf{W}$  with support  $S$  and PDF  $f(\mathbf{w})$ . Namely,  $h(\mathbf{W}) := -\int_S f(\mathbf{w}) \log f(\mathbf{w}) d\mathbf{w}$ , where  $\log(\cdot)$  denotes the natural logarithm function throughout this paper. Two things to note here:

- i) The capacity  $C$  and its bounds in this paper are all measured in the unit of nats.
- ii) By an abuse of notation, we allow the argument of  $h(\cdot)$  to be a random vector, a PDF  $f$ , or the name of a distribution such as VDFAP. For instance, we can write  $h(f) = -\int_S f(\mathbf{w}) \log f(\mathbf{w}) d\mathbf{w}$  to denote the differential entropy of a distribution with PDF  $f$ , when the support  $S$  is clear from the context.

For  $d = 1$ , to our best knowledge, no closed-form expression for the differential entropy of VDFAP<sup>(1)</sup>( $u, \lambda$ ) is known. However, for  $d = 2$ , we have calculated the differential entropy of a random vector  $\mathbf{N}$  following VDFAP<sup>(2)</sup>( $u, \lambda$ ) in closed-form [2, Appendix B]:

$$h(\mathbf{N}) = \log(2\pi e^3) + 2\log(\lambda) - \log(1 + \lambda|u|) - \lambda|u|e^{\lambda|u|}(e \cdot \text{Ei}(-1 - \lambda|u|) - 3 \cdot \text{Ei}(-\lambda|u|)), \quad (36)$$

where the exponential integral function  $\text{Ei}(\cdot)$  is defined as [31]:

$$\text{Ei}(x) := -\int_{-x}^{\infty} \frac{e^{-t}}{t} dt, \text{ for } x < 0. \quad (37)$$

#### A. Lower Bound

Using the weak stability property of VDFAP distributions proved in Section IV-B, we obtain a lower bound on the capacity (34) of the VDFAP channel:

$$C^{(d)}(u, \lambda, \Sigma) \geq h(\text{VDFAP}^{(d)}(u, \lambda + |u|\sigma_{\min}(\Sigma))) - h(\text{VDFAP}^{(d)}(u, \lambda)), \quad (38)$$

where  $\sigma_{\min}(\cdot)$  denotes the minimum eigenvalue of its argument. Specifically, when  $d = 2$ , we have a closed-form lower bound:

$$\begin{aligned}
C^{(2)}(u, \lambda, \Sigma) &\geq 2 \log \left( 1 + \frac{|u|}{\lambda} \sigma_{\min}(\Sigma) \right) - \log \left( 1 + \frac{|u|^2}{1 + \lambda|u|} \sigma_{\min}(\Sigma) \right) \\
&\quad + \lambda|u|e^{\lambda|u|} \left( e \cdot \text{Ei}(-1 - \lambda|u|) - 3 \cdot \text{Ei}(-\lambda|u|) \right) \\
&\quad - \left( \lambda + |u|\sigma_{\min}(\Sigma) \right) |u| \exp \{ (\lambda + |u|\sigma_{\min}(\Sigma)) |u| \} \\
&\quad \times \left\{ e \cdot \text{Ei} \left( -1 - (\lambda + |u|\sigma_{\min}(\Sigma)) |u| \right) - 3 \cdot \text{Ei} \left( -(\lambda + |u|\sigma_{\min}(\Sigma)) |u| \right) \right\} \\
&> 0.
\end{aligned} \tag{39}$$

*Proof:* To obtain a lower bound on the capacity, we pick particular input distributions  $f(\mathbf{X})$  satisfying the second-moment constraint  $\mathbb{E} [\mathbf{X} \mathbf{X}^\top] \preceq \Sigma$ , calculate  $h(\mathbf{Y}) - h(\mathbf{N})$ , and then optimize the result via taking supremum.

Take  $\mathbf{X} \sim \text{VDFAP}^{(d)}(u, \lambda')$  for some strictly positive  $\lambda' \leq |u|\sigma_{\min}(\Sigma)$ . By (32), we have that  $\mathbb{E} [\mathbf{X} \mathbf{X}^\top] = \frac{\lambda'}{|u|} \mathbb{I}_d \preceq \sigma_{\min}(\Sigma) \mathbb{I}_d \preceq \Sigma$ , so  $\mathbf{X}$  satisfies the covariance constraint. Also, by the *weak stability property* proved in Section IV-B,  $\mathbf{Y} = \mathbf{X} + \mathbf{N}$  follows  $\text{VDFAP}^{(d)}(u, \lambda + \lambda')$ . Then, a lower bound that holds for any  $0 < \lambda' \leq |u|\sigma_{\min}(\Sigma)$  is:

$$C^{(d)}(u, \lambda, \Sigma) \geq h(\mathbf{Y}) - h(\mathbf{N}) = h(\text{VDFAP}^{(d)}(u, \lambda + \lambda')) - h(\text{VDFAP}^{(d)}(u, \lambda)), \tag{40}$$

which follows from (35). Taking  $\lambda' = |u|\sigma_{\min}(\Sigma)$  proves (38).

To obtain the closed-form expression for the lower bound in (39) when  $d = 2$ , we introduce an ancillary function  $h_0 : \mathbb{R}^+ \rightarrow \mathbb{R}$  defined by

$$h_0(s) := 2 \log(s) - \log(1 + s) - s e^s (e \cdot \text{Ei}(-1 - s) - 3 \cdot \text{Ei}(-s)), \text{ for } s > 0, \tag{41}$$

so that the differential entropy (36) of a random vector  $\mathbf{Z} \sim \text{VDFAP}^{(2)}(u, \lambda'')$  can be expressed as  $h(\mathbf{Z}) = h_0(|u|\lambda'') + \log(2\pi e^3) - 2 \log(|u|)$ . Therefore, the lower bound (40) can be expressed via the function  $h_0(\cdot)$  as

$$C^{(2)}(u, \lambda, \Sigma) \geq h_0(|u|(\lambda + \lambda')) - h_0(|u|\lambda), \quad \forall 0 < \lambda' \leq |u|\sigma_{\min}(\Sigma). \tag{42}$$

Hence, we can maximize over  $\lambda'$  to get a tighter bound:

$$C^{(2)}(u, \lambda, \Sigma) \geq \sup_{0 < \lambda' \leq |u| \sigma_{\min}(\Sigma)} h_0(|u|(\lambda + \lambda')) - h_0(|u|\lambda). \quad (43)$$

It is shown in [2, Appendix C] that  $h_0(\cdot)$  is strictly monotonically increasing. Therefore, (43) boils down to plugging the maximum  $\lambda'$ , i.e.,  $|u| \sigma_{\min}(\Sigma)$ , into (42):

$$C^{(2)}(u, \lambda, \Sigma) \geq h_0\left(|u|\left(\lambda + |u| \sigma_{\min}(\Sigma)\right)\right) - h_0(|u|\lambda) > 0. \quad (44)$$

The strict positivity of the lower bound in (44) follows from the monotonicity of  $h_0(\cdot)$  and that  $\sigma_{\min}(\Sigma) > 0$  as  $\Sigma \succ 0$ .

Last but not least, the closed-form lower bound in (39) can be obtained by directly plugging the expression (41) of  $h_0$  into the lower bound in (44). The lower bound in (39) is also strictly positive due to the same argument. ■

## B. Upper Bound

It is well-established in the literature that the differential entropy is maximized by multivariate Gaussian under a prescribed correlation matrix [39]. This fact can be generalized to a larger family of distributions satisfying a covariance constraint of the form in (34) [40, Theorem 2.7]. Thus, this generalization can be applied to establish an upper bound on the capacity (34), which can be expressed as:

$$C^{(d)}(u, \lambda, \Sigma) \leq \frac{1}{2 \log(2)} \log \left( (2\pi e)^d \det \left( \Sigma + \frac{\lambda}{|u|} \mathbb{I}_d \right) \right) - h(\text{VDFAP}^{(d)}(u, \lambda)), \quad (45)$$

where  $\det(\cdot)$  denotes the determinant function. Specifically, when  $d = 2$ , we have a closed-form upper bound:

$$\begin{aligned} C^{(2)}(u, \lambda, \Sigma) &\leq \frac{1}{2 \log(2)} \log \left( \det \left( \Sigma + \frac{\lambda}{|u|} \mathbb{I}_2 \right) \right) - 2 \log(\lambda) + \log(1 + \lambda|u|) \\ &\quad + \lambda|u| e^{\lambda|u|} (e \cdot \text{Ei}(-1 - \lambda|u|) - 3 \cdot \text{Ei}(-\lambda|u|)) \\ &\quad + \left( \frac{1}{\log(2)} - 1 \right) \log(2\pi e) - 2. \end{aligned} \quad (46)$$

*Proof:* Consider (35) as the maximization problem

$$C = \max_{f(\mathbf{X}) \in \mathcal{F}_\Sigma} h(\mathbf{X} + \mathbf{N}) - h(\mathbf{N}) \quad (47)$$

where the constraint set  $\mathcal{F}_\Sigma$  is the family of input distributions  $\mathcal{F}_\Sigma = \{f(\mathbf{X}) : \mathbb{E}[\mathbf{X}\mathbf{X}^\top] \preceq \Sigma\}$ .

We can calculate the output correlation matrix as

$$\begin{aligned} \mathbb{E}[\mathbf{Y}\mathbf{Y}^\top] &= \mathbb{E}[(\mathbf{X} + \mathbf{N})(\mathbf{X} + \mathbf{N})^\top] \\ &\stackrel{(a)}{=} \mathbb{E}[\mathbf{X}\mathbf{X}^\top] + \mathbb{E}[\mathbf{X}]\mathbb{E}[\mathbf{N}]^\top + \mathbb{E}[\mathbf{N}]\mathbb{E}[\mathbf{X}]^\top + \mathbb{E}[\mathbf{N}\mathbf{N}^\top] \\ &\stackrel{(b)}{=} \mathbb{E}[\mathbf{X}\mathbf{X}^\top] + \mathbb{E}[\mathbf{N}\mathbf{N}^\top] \\ &\stackrel{(c)}{=} \mathbb{E}[\mathbf{X}\mathbf{X}^\top] + \frac{\lambda}{|u|}\mathbb{I}_d, \end{aligned} \quad (48)$$

where (a) is due to the independence of  $\mathbf{X}$  and  $\mathbf{N}$ , (b) is due to  $\mathbb{E}[\mathbf{N}] = \mathbf{0}$  and (c) is due to (32). Because of (48), we have that the maximization problem (47) is equivalent to the following

$$C = \max_{f(\mathbf{Y}) \in \mathcal{F}_{\Sigma'}} h(\mathbf{Y}) - h(\mathbf{N}), \quad (49)$$

where we denoted  $\Sigma' = \Sigma + \frac{\lambda}{|u|}\mathbb{I}_d$  and the family of output distributions as:

$$\mathcal{F}_{\Sigma'} = \{f(\mathbf{Y}) : \mathbb{E}[\mathbf{Y}\mathbf{Y}^\top] \preceq \Sigma'\}. \quad (50)$$

Under the covariance constraint (50) on the output  $\mathbf{Y}$ , its differential entropy  $h(\mathbf{Y})$  is maximized when  $\mathbf{Y}$  follows the Gaussian distribution  $\mathcal{N}(\mathbf{0}, \Sigma')$  [40, Theorem 2.7]:

$$\max_{f(\mathbf{Y}) \in \mathcal{F}_{\Sigma'}} h(\mathbf{Y}) = h(\mathcal{N}(\mathbf{0}, \Sigma')) \quad (51)$$

$$= \frac{1}{2 \log(2)} \log((2\pi e)^d \det(\Sigma')). \quad (52)$$

To conclude, from (49) and (51) we have

$$C \leq h\left(\mathcal{N}\left(\mathbf{0}, \Sigma + \frac{\lambda}{|u|}\mathbb{I}_d\right)\right) - h(\text{VDFAP}^{(d)}(u, \lambda)), \quad (53)$$

which yields (45) after applying (52). To get a closed-form upper bound when  $d = 2$ , we plug the differential entropy expression (36) into (45) and simplify to get (46). ■

## VI. CONCLUSION

In this paper, we explored two fundamental problems in the field of diffusive molecular communication (MC): characterization of the first arrival position (FAP) density and the capacity bounding problem of vertically-drifted FAP channels.

We first presented a unified approach to the FAP density characterization problem for MC systems with a fully-absorbing receiver. Our approach establishes a connection between (macroscopic) partial differential equation models and (microscopic) stochastic differential equation models. Using stochastic analysis tools, we proposed a concise expression, represented by (23), which relates the FAP density to the elliptic-type Green's function. Notably, this expression is applicable to any spatial dimension, drift direction, and receiver shape.

In addition, we demonstrated (in Appendix A) the effectiveness of our approach by providing special case calculations: the 2D linear receiver, the 3D planar receiver, and the 3D spherical receiver. We showed that our approach can precisely reproduce known results on FAP density in the literature. Moreover, for the 2D linear receiver case, our approach improves upon the existing formula by accommodating arbitrary drift directions.

Having access to the explicit forms of FAP density, we are able to conduct a more comprehensive analysis of the proposed MC system, which utilizes position information. In particular, we addressed the problem of bounding the capacity of vertically-drifted FAP channels under the covariance (matrix) constraint.

Drawing inspiration from vector Gaussian interference channels, we provided closed-form upper and lower bounds on this capacity in the three-dimensional setting. This was achieved through a detailed analysis of the characteristic function of vertically-drifted FAP noise distributions, which also led to the discovery of a novel weak stability property intrinsic to vertically-drifted FAP noise distributions.

Our findings contribute to the ongoing efforts to comprehend the fundamental limits of

molecular communication systems. They also open new avenues for future research, including extending the analysis to other spatial dimensions, exploring the implications of the discovered weak stability property, and investigating other settings beyond the vertically-drifted case.

## APPENDIX A

### CALCULATING FAP DENSITY IN SPECIFIC SCENARIOS

This section outlines the application of formula (23) and the novel methodology presented in Section III to compute the FAP density in practical scenarios that are relevant to MC.

#### A. 2D Linear Receiver and 3D Planar Receiver

In this subsection, we unify the FAP density calculation for 2D linear receivers and 3D planar receivers by employing the innovative approach introduced in Section III.

To calculate the  $d$ -dimensional FAP density, we consider an Itô diffusion  $\mathbf{X}_t \in \mathbb{R}^D$  with a semigroup generator  $A := \sum_{i=1}^D v_i \frac{\partial}{\partial x_i} + \frac{\sigma^2}{2} \sum_{i=1}^D \frac{\partial^2}{\partial x_i^2}$  (recall  $d := D - 1$ ). We denote the Laplacian operator [27] in  $D$  dimensions by  $\Delta_D$  and consider the following drift-diffusion BVP in Cartesian coordinates:

$$\begin{cases} A\phi = \sum_{i=1}^D v_i \frac{\partial \phi}{\partial x_i} + \frac{\sigma^2}{2} \Delta_D \phi = 0 & \text{in } \Omega \\ \phi = g & \text{on } \partial\Omega \end{cases}, \quad (54)$$

where  $\phi$  is a (dummy) unknown function,  $\Omega = \mathbb{R}^D \cap \{x_D > 0\}$  is the domain of (54), and  $\partial\Omega = \mathbb{R}^D \cap \{x_D = 0\}$  is the boundary of the domain. Here, we use the notation  $x_j$  to indicate the  $j$ -th component of the position vector  $\mathbf{x} = [x_1, \dots, x_D]^\top$  in an  $D$ -dimensional space. We temporarily set  $\sigma^2 = 1$ , and then treat the general case later.

To simplify the problem further, we introduce a change of variable  $\psi(\mathbf{x}) = \gamma(\mathbf{x})\phi(\mathbf{x})$ . The *drift factor*  $\gamma(\cdot)$  is defined as  $\gamma(\mathbf{x}) := \exp\{\mathbf{v}^\top \mathbf{x}\}$ , which depends only on the drift components. After changing the variables, we obtain a new BVP with the same  $\Omega$  as

$$\begin{cases} \tilde{A}(\psi) = \Delta_D \psi - s^2 \psi = 0 & \text{in } \Omega \\ \psi = \tilde{g} & \text{on } \partial\Omega \end{cases}, \quad (55)$$



where  $s = \|\mathbf{v}\|$  denotes the magnitude of the drift vector. This new operator  $\tilde{A}$  is called the Helmholtz operator in the literature [33], so we call this new BVP (55) the Helmholtz BVP.

According to [33], for both  $D = 2$  and  $D = 3$ , the solution to the Helmholtz BVP (55) can be compactly written as

$$\psi(\mathbf{x}) = \int_{\mathbf{y} \in \partial\Omega} \left| \frac{\partial \tilde{G}(\mathbf{x}, \mathbf{y})}{\partial \mathbf{n}_{\mathbf{y}}} \right| \tilde{g}(\mathbf{y}) \, d\mathbf{y}, \quad (56)$$

where the notation  $\left| \frac{\partial \tilde{G}(\mathbf{x}, \mathbf{y})}{\partial \mathbf{n}_{\mathbf{y}}} \right|$  denotes the absolute value of the directional derivative of  $\tilde{G}$  with respect to the outward normal on the boundary  $\partial\Omega$ . The Green's function<sup>5</sup>  $\tilde{G}$  corresponding to Helmholtz BVP (55) is known and can be separately written down for  $D = 2$  and  $D = 3$ .

In order to obtain a representation formula for the solution  $\phi$  of the original BVP (54), we substitute  $\psi(\mathbf{x}) = \gamma(\mathbf{x})\phi(\mathbf{x})$  back into (56), yielding

$$\begin{aligned} \phi(\mathbf{x}) &= \frac{\psi(\mathbf{x})}{\gamma(\mathbf{x})} = \exp\{-\mathbf{v}^\top \mathbf{x}\} \int_{\partial\Omega} \left| \frac{\partial \tilde{G}(\mathbf{x}, \mathbf{y})}{\partial \mathbf{n}_{\mathbf{y}}} \right| \tilde{g}(\mathbf{y}) \, d\mathbf{y} \\ &\stackrel{(a)}{=} \int_{\partial\Omega} \exp\{\mathbf{v}^\top \mathbf{y} - \mathbf{v}^\top \mathbf{x}\} \left| \frac{\partial \tilde{G}(\mathbf{x}, \mathbf{y})}{\partial \mathbf{n}_{\mathbf{y}}} \right| g(\mathbf{y}) \, d\mathbf{y} \quad . \\ &\stackrel{(b)}{=} \int_{\partial\Omega} \mathcal{K}_{\mathbf{v}}(\mathbf{x}, \mathbf{y}) g(\mathbf{y}) \, d\mathbf{y} \end{aligned} \quad (57)$$

In (a), we have used a relation between the boundary data before and after the change of variable:  $\tilde{g}(\mathbf{y}) = e^{\mathbf{v}^\top \mathbf{y}} g(\mathbf{y})$ . In (b), we use the notation  $\mathcal{K}_{\mathbf{v}}(\mathbf{x}, \mathbf{y})$  to represent the overall integral kernel (see the definition of this term in [27]). Note that this integral kernel can be also expressed by  $\left| \frac{\partial G(\mathbf{x}, \mathbf{y})}{\partial \mathbf{n}_{\mathbf{y}}} \right|$ , where  $G$  corresponds to the Green's function of original BVP (54). From (57), we see that

$$\left| \frac{\partial G(\mathbf{x}, \mathbf{y})}{\partial \mathbf{n}_{\mathbf{y}}} \right| = \mathcal{K}_{\mathbf{v}}(\mathbf{x}, \mathbf{y}) = \exp\{\mathbf{v}^\top (\mathbf{y} - \mathbf{x})\} \left| \frac{\partial \tilde{G}(\mathbf{x}, \mathbf{y})}{\partial \mathbf{n}_{\mathbf{y}}} \right|. \quad (58)$$

In the following, we separately write down, for  $D = 2$  and  $D = 3$ , the Green's function  $\tilde{G}$  corresponding to Helmholtz BVP (55) from [33] and explicitly carry out the calculation in (58).

<sup>5</sup>We use  $\tilde{G}$  to emphasize that this is the Green's function corresponding to the Helmholtz BVP, not to the original BVP.

1) *2D Linear Receiver*: According to [33], when  $D = 2$ , the Green's function corresponding to Helmholtz BVP (55) has the form

$$\tilde{G}(\mathbf{x}, \mathbf{y}) = \tilde{G}(x_1, x_2, \xi, \eta) = \frac{1}{2\pi} [K_0(s\rho_1) - K_0(s\rho_2)], \quad (59)$$

where  $\mathbf{x} = [x_1, x_2]^\top$  and  $\mathbf{y} = [\xi, \eta]^\top$  are general positions in 2D, and we have defined  $\rho_1 := \sqrt{(x_1 - \xi)^2 + (x_2 - \eta)^2}$  and  $\rho_2 := \sqrt{(x_2 - \xi)^2 + (x_2 + \eta)^2}$ . From (59), we can directly calculate

$$\left| \frac{\partial \tilde{G}(\mathbf{x}, \mathbf{y})}{\partial \mathbf{n}_{\mathbf{y}}} \right|_{\partial\Omega} = \left[ \frac{\partial \tilde{G}}{\partial \rho_1} \frac{\partial \rho_1}{\partial \eta} + \frac{\partial \tilde{G}}{\partial \rho_2} \frac{\partial \rho_2}{\partial \eta} \right]_{\eta=0} = \frac{s\lambda}{\pi} \frac{K_1 \left( s \sqrt{(x_1 - \xi)^2 + \lambda^2} \right)}{\sqrt{(x_1 - \xi)^2 + \lambda^2}}, \quad (60)$$

where we have specified the emission point  $\mathbf{x} = [x_1, \lambda]^\top$  as well as the arrival point  $\mathbf{y} = [\xi, 0]^\top$  hereafter for the 2D linear receiver. Notice that  $\mathbf{y}$  now lies on the boundary  $\partial\Omega$ . The parameter  $\lambda > 0$  is the distance from the emission point to the linear receiver, as illustrated in Fig. 1. Then according to (58) and  $s = \|\mathbf{v}\|$ , we obtain

$$\left| \frac{\partial G(\mathbf{x}, \mathbf{y})}{\partial \mathbf{n}_{\mathbf{y}}} \right|_{\partial\Omega} = \mathcal{K}_{\mathbf{v}}(\mathbf{x}, \mathbf{y}) \Big|_{\partial\Omega} = \exp \{ \mathbf{v}^\top (\mathbf{y} - \mathbf{x}) \} \frac{\|\mathbf{v}\| \lambda}{\pi} \frac{K_1 (\|\mathbf{v}\| \|\mathbf{y} - \mathbf{x}\|)}{\|\mathbf{y} - \mathbf{x}\|}, \quad (61)$$

where we have substituted  $\|\mathbf{y} - \mathbf{x}\| = \sqrt{(x_1 - \xi)^2 + \lambda^2}$  into (60). This  $\mathcal{K}_{\mathbf{v}}(\mathbf{x}, \mathbf{y}) \Big|_{\partial\Omega}$  is just the desired FAP density according to relation (23) presented in Section III. We will denote this integral kernel by  $f_{\mathbf{Y}|\mathbf{X}}(\mathbf{y}|\mathbf{x})$  hereafter.

For the general case  $\sigma^2 \neq 1$ , we only need to replace  $v_i$  with  $\frac{v_i}{\sigma^2} = u_i$  (recall  $\mathbf{u} := \frac{\mathbf{v}}{\sigma^2}$ ), yielding the desired FAP density that allows arbitrary drift directions:

$$f_{\mathbf{Y}|\mathbf{X}}(\mathbf{y}|\mathbf{x}) = \frac{\|\mathbf{u}\| \lambda}{\pi} \exp \{ \mathbf{u}^\top (\mathbf{y} - \mathbf{x}) \} \frac{K_1 (\|\mathbf{u}\| \|\mathbf{y} - \mathbf{x}\|)}{\|\mathbf{y} - \mathbf{x}\|}. \quad (62)$$

Equation (62) is a new formula in the MC field. Setting  $v_1 = 0$  in (62) recovers the restrictive version in [19]:

$$f_{\mathbf{Y}|\mathbf{X}}(\mathbf{y}|\mathbf{x}) = \frac{|v_2| \lambda}{2\pi D} \exp \left\{ \frac{-v_2 \lambda}{2D} \right\} \frac{K_1 \left( \frac{|v_2|}{2D} \sqrt{(x_1 - \xi)^2 + \lambda^2} \right)}{\sqrt{(x_1 - \xi)^2 + \lambda^2}}, \quad (63)$$

where we have used the relation  $\sigma^2 = 2D$ .<sup>6</sup> To conclude, our formula (62) improves the formula [19, eq. (19)] by allowing arbitrary drift directions.

2) *3D Planar Receiver*: According to [33], when  $D = 3$ , the Green's function corresponding to Helmholtz BVP (55) has the form:

$$\tilde{G}(\mathbf{x}, \mathbf{y}) = \tilde{G}(x_1, x_2, x_3, \xi, \eta, \zeta) = \frac{\exp(-s\mathcal{R}_1)}{4\pi\mathcal{R}_1} - \frac{\exp(-s\mathcal{R}_2)}{4\pi\mathcal{R}_2}, \quad (64)$$

where  $\mathbf{x} = [x_1, x_2, x_3]^\top$  and  $\mathbf{y} = [\xi, \eta, \zeta]^\top$  are general positions in 3D, and we have defined  $\mathcal{R}_1 := \sqrt{(x_1 - \xi)^2 + (x_2 - \eta)^2 + (x_3 - \zeta)^2}$  and  $\mathcal{R}_2 := \sqrt{(x_1 - \xi)^2 + (x_2 - \eta)^2 + (x_3 + \zeta)^2}$ .

From (64), we can directly differentiate to get

$$\left| \frac{\partial \tilde{G}(\mathbf{x}, \mathbf{y})}{\partial \mathbf{n}_\mathbf{y}} \right|_{\partial\Omega} = \left[ \frac{\partial}{\partial \zeta} \tilde{G}(x_1, x_2, x_3, \xi, \eta, \zeta) \right]_{\zeta=0} = \frac{\lambda}{2\pi} \exp\{-s\|\mathbf{y} - \mathbf{x}\|\} \left[ \frac{1 + s\|\mathbf{y} - \mathbf{x}\|}{\|\mathbf{y} - \mathbf{x}\|^3} \right] \quad (65)$$

where we have specified the emission point  $\mathbf{x} = [x_1, x_2, \lambda]^\top$  and the arrival point  $\mathbf{y} = [\xi, \eta, 0]^\top$  hereafter for the 3D planar receiver. Notice that  $\mathbf{y}$  now lies on the boundary  $\partial\Omega$ . The parameter  $\lambda > 0$  is the distance from the emission point to the planar receiver, as illustrated in Fig. 2.

Then according to (58) and  $s = \|\mathbf{v}\|$ , we obtain

$$\begin{aligned} \left| \frac{\partial G(\mathbf{x}, \mathbf{y})}{\partial \mathbf{n}_\mathbf{y}} \right|_{\partial\Omega} &= \mathcal{K}_\mathbf{v}(\mathbf{x}, \mathbf{y}) \Big|_{\partial\Omega} \\ &= \exp\{\mathbf{v}^\top(\mathbf{y} - \mathbf{x})\} \frac{\lambda}{2\pi} \exp\{-\|\mathbf{v}\|\|\mathbf{y} - \mathbf{x}\|\} \left[ \frac{1 + \|\mathbf{v}\|\|\mathbf{y} - \mathbf{x}\|}{\|\mathbf{y} - \mathbf{x}\|^3} \right]. \end{aligned} \quad (66)$$

This integral kernel  $\mathcal{K}_\mathbf{v}(\mathbf{x}, \mathbf{y}) \Big|_{\partial\Omega}$  can be interpreted as the probability density function of the FAP (see (23), Section III), so we denote it by  $f_{\mathbf{Y}|\mathbf{X}}(\mathbf{y}|\mathbf{x})$  hereafter.

Lastly, to treat the general case  $\sigma^2 \neq 1$ , we can simply replace  $v_i$  with  $\frac{v_i}{\sigma^2} = u_i$  (recall  $\mathbf{u} := \frac{\mathbf{v}}{\sigma^2}$ ).

This yields:

$$f_{\mathbf{Y}|\mathbf{X}}(\mathbf{y}|\mathbf{x}) = \frac{\lambda}{2\pi} \exp\{\mathbf{u}^\top(\mathbf{y} - \mathbf{x})\} \exp\{-\|\mathbf{u}\|\|\mathbf{y} - \mathbf{x}\|\} \left[ \frac{1 + \|\mathbf{u}\|\|\mathbf{y} - \mathbf{x}\|}{\|\mathbf{y} - \mathbf{x}\|^3} \right]. \quad (67)$$

Equation (67) is the desired 3D FAP density function, allowing arbitrary drift directions.

<sup>6</sup>In the literature, the diffusion coefficient  $D$  may have different definitions, which can vary by a constant factor. However, the unit of  $D$  consistently corresponds to  $\sigma^2$ .

### B. 3D Spherical Receiver

In this subsection, we tackle the 3D spherical receiver case with the assumption of zero drift velocity, the same setting as in [16]. Note that the result we are going to show is already known in the literature, so we present a very brief version of how to obtain the angular density using our proposed methodology. The main goal of this subsection is to demonstrate the capability of our method to handle receivers with various shapes.

We consider an Itô diffusion  $\mathbf{X}_t \in \mathbb{R}^3$  with zero drift, i.e., all  $v_i = 0$ . The corresponding generator  $A$  is simply the 3D Laplacian operator. It is well known that the 3D Laplace equation in the spherical coordinate [27] can be expressed as

$$\frac{1}{r^2} \frac{\partial}{\partial r} \left( r^2 \frac{\partial \phi}{\partial r} \right) + \frac{1}{r^2 \sin \theta} \frac{\partial}{\partial \theta} \left( \sin \theta \frac{\partial \phi}{\partial \theta} \right) + \frac{1}{r^2 \sin^2 \theta} \frac{\partial^2 \phi}{\partial \varphi^2} = 0, \quad (68)$$

where  $r = \sqrt{x^2 + y^2 + z^2}$ . Assuming a prescribed boundary data  $g(\theta, \varphi)$  at the surface ( $r = R$ ) of the spherical receiver with radius  $R > 0$ , i.e.,  $\phi = g(\theta, \varphi)$  at  $r = R$ , the solution of the outer problem for  $r \geq R$  can be obtained as [33, Section 8.1.3]:

$$\phi(r, \theta, \varphi) = \frac{R}{4\pi} \int_0^{2\pi} \int_0^\pi g(\theta_0, \varphi_0) \cdot \frac{r^2 - R^2}{(r^2 - 2rR \cdot \kappa(\theta, \varphi; \theta_0, \varphi_0) + R^2)^{3/2}} \sin \theta_0 \, d\theta_0 \, d\varphi_0, \quad (69)$$

where  $\kappa(\theta, \varphi; \theta_0, \varphi_0) := \cos \theta \cos \theta_0 + \sin \theta \sin \theta_0 \cos(\varphi - \varphi_0)$ .

A comparison between formula (69) and equation (22) allows us to determine  $\left| \frac{\partial G}{\partial \mathbf{n}_y}(\mathbf{x}, \mathbf{y}) \right|$ , which is exactly the FAP density  $f_{\mathbf{Y}|\mathbf{X}}(\mathbf{y}|\mathbf{x})$  due to our proposed formula (23). That is, we have already obtained the (marginal) *angular density* of the hitting position of molecules, which was expressed in [16, eq. (3)-(4)] and [22, eq. (6.3.3a)]. This demonstrates the versatility of our FAP calculating methodology in handling various receiver shapes, including spherical receivers.

## REFERENCES

- [1] Y.-C. Lee, J.-M. Wu, and M.-H. Hsieh, "A unified framework for calculating first arrival position density in molecular communication," arXiv:2201.04476v3 [cs.IT], Apr. 2023.
- [2] Y.-F. Lo, Y.-C. Lee, and M.-H. Hsieh, "Capacity bounds for vertically-drifted first arrival position channels under a covariance constraint," arXiv:2305.02706v4 [cs.IT], May 2023.

- [3] T. Nakano, A. W. Eckford, and T. Haraguchi, *Molecular Communication*. Cambridge University Press, 2013.
- [4] W. Guo, C. Mias, N. Farsad, and J.-L. Wu, “Molecular versus electromagnetic wave propagation loss in macro-scale environments,” *IEEE Transactions on Molecular, Biological and Multi-Scale Communications*, vol. 1, no. 1, pp. 18–25, 2015.
- [5] I. F. Akyildiz, F. Brunetti, and C. Blázquez, “Nanonetworks: A new communication paradigm,” *Computer Networks*, vol. 52, no. 12, pp. 2260–2279, 2008.
- [6] M. Pierobon and I. F. Akyildiz, “A physical end-to-end model for molecular communication in nanonetworks,” *IEEE Journal on Selected Areas in Communications*, vol. 28, no. 4, pp. 602–611, 2010.
- [7] N. Farsad, H. B. Yilmaz, A. Eckford, C.-B. Chae, and W. Guo, “A comprehensive survey of recent advancements in molecular communication,” *IEEE Communications Surveys & Tutorials*, vol. 18, no. 3, pp. 1887–1919, 2016.
- [8] M. Pierobon and I. F. Akyildiz, “Capacity of a diffusion-based molecular communication system with channel memory and molecular noise,” *IEEE Transactions on Information Theory*, vol. 59, no. 2, pp. 942–954, 2012.
- [9] S. Kadloor, R. S. Adve, and A. W. Eckford, “Molecular communication using Brownian motion with drift,” *IEEE Transactions on NanoBioscience*, vol. 11, no. 2, pp. 89–99, 2012.
- [10] M. Moore, A. Enomoto, T. Nakano, R. Egashira, T. Suda, A. Kayasuga, H. Kojima, H. Sakakibara, and K. Oiwa, “A design of a molecular communication system for nanomachines using molecular motors,” in *Proc. 4th Annu. IEEE Int. Conf. Pervasive Comput. Commun. Workshops (PERCOMW)*, Pisa, Italy, Mar. 2006, pp. 554–559.
- [11] D. Bi, Y. Deng, M. Pierobon, and A. Nallanathan, “Chemical reactions-based microfluidic transmitter and receiver design for molecular communication,” *IEEE Transactions on Communications*, vol. 68, no. 9, pp. 5590–5605, 2020.
- [12] M. Ş. Kuran, H. B. Yilmaz, I. Demirkol, N. Farsad, and A. Goldsmith, “A survey on modulation techniques in molecular communication via diffusion,” *IEEE Communications Surveys & Tutorials*, vol. 23, no. 1, pp. 7–28, 2020.
- [13] V. Jamali, A. Ahmadzadeh, W. Wicke, A. Noel, and R. Schober, “Channel modeling for diffusive molecular communication—a tutorial review,” *Proceedings of the IEEE*, vol. 107, no. 7, pp. 1256–1301, 2019.
- [14] A. Noel, Y. Deng, D. Makrakis, and A. Hafid, “Active versus passive: receiver model transforms for diffusive molecular communication,” in *2016 IEEE Global Communications Conference (GLOBECOM)*. IEEE, 2016, pp. 1–6.
- [15] H. B. Yilmaz, A. C. Heren, T. Tugcu, and C.-B. Chae, “Three-dimensional channel characteristics for molecular communications with an absorbing receiver,” *IEEE Communications Letters*, vol. 18, no. 6, pp. 929–932, 2014.
- [16] B. C. Akdeniz, N. A. Turgut, H. B. Yilmaz, C.-B. Chae, T. Tugcu, and A. E. Pusane, “Molecular signal modeling of a partially counting absorbing spherical receiver,” *IEEE Transactions on Communications*, vol. 66, no. 12, pp. 6237–6246, 2018.
- [17] K. V. Srinivas, A. W. Eckford, and R. S. Adve, “Molecular communication in fluid media: The additive inverse Gaussian noise channel,” *IEEE Transactions on Information Theory*, vol. 58, no. 7, pp. 4678–4692, 2012.
- [18] Y.-C. Lee, C.-C. Chen, P.-C. Yeh, and C.-H. Lee, “Distribution of first arrival position in molecular communication,” in *Proc. IEEE Int. Symp. Information Theory*, Barcelona, Spain, July 2016, pp. 1033–1037.

- [19] N. Pandey, R. K. Mallik, and B. Lall, “Molecular communication: The first arrival position channel,” *IEEE Wireless Communications Letters*, vol. 8, no. 2, pp. 508–511, 2018.
- [20] H. Li, S. M. Moser, and D. Guo, “Capacity of the memoryless additive inverse Gaussian noise channel,” *IEEE Journal on Selected Areas in Communications*, vol. 32, no. 12, pp. 2315–2329, 2014.
- [21] N. Farsad, Y. Murin, A. Eckford, and A. Goldsmith, “On the capacity of diffusion-based molecular timing channels,” in *2016 IEEE International Symposium on Information Theory (ISIT)*. IEEE, 2016, pp. 1023–1027.
- [22] S. Redner, *A Guide to First-Passage Processes*. Cambridge University Press, 2001.
- [23] J. D. Jackson, *Classical Electrodynamics*, 3rd ed. Wiley, 1998.
- [24] A. W. Eckford, K. Srinivas, and R. S. Adve, “The peak constrained additive inverse Gaussian noise channel,” in *Proc. IEEE Int. Symp. Information Theory*, Cambridge, MA, USA, July 2012, pp. 2983–2987.
- [25] H.-T. Chang and S. M. Moser, “Bounds on the capacity of the additive inverse Gaussian noise channel,” in *Proc. IEEE Int. Symp. Information Theory*, Cambridge, MA, USA, July 2012, pp. 299–303.
- [26] X. Shang, B. Chen, G. Kramer, and H. V. Poor, “Capacity regions and sum-rate capacities of vector Gaussian interference channels,” *IEEE Transactions on Information Theory*, vol. 56, no. 10, pp. 5030–5044, 2010.
- [27] D. G. Zill, *Advanced Engineering Mathematics*. Jones & Bartlett Learning, 2020.
- [28] B. Øksendal, *Stochastic Differential Equations: An Introduction with Applications*. Springer Science & Business Media, 2013.
- [29] O. Calin, *An Informal Introduction to Stochastic Calculus with Applications*. World Scientific, 2015.
- [30] N. Farsad, W. Guo, C.-B. Chae, and A. Eckford, “Stable distributions as noise models for molecular communication,” in *2015 IEEE Global Communications Conference (GLOBECOM)*, 2015, pp. 1–6.
- [31] I. S. Gradshteyn and I. M. Ryzhik, *Table of Integrals, Series, and Products*. Academic Press, 2014.
- [32] M. H. Stone, “On one-parameter unitary groups in Hilbert space,” *Annals of Mathematics*, pp. 643–648, 1932.
- [33] A. D. Polyanin, *Handbook of Linear Partial Differential Equations for Engineers and Scientists*. Chapman and hall/crc, 2001.
- [34] S. E. Shreve *et al.*, *Stochastic Calculus for Finance II: Continuous-Time Models*. Springer, 2004, vol. 11.
- [35] R. Durrett, *Probability: Theory and Examples*. Cambridge University Press, 2019.
- [36] S. Kotz and S. Nadarajah, *Multivariate t-distributions and Their Applications*. Cambridge University Press, 2004.
- [37] E. Lukacs, *Characteristic Function*. Charles Griffin & Company Limited, 1970.
- [38] H. Fallahgoul, S. Hashemiparast, F. J. Fabozzi, and Y. S. Kim, “Multivariate stable distributions and generating densities,” *Applied Mathematics Letters*, vol. 26, no. 3, pp. 324–329, 2013.
- [39] T. M. Cover, *Elements of Information Theory*. John Wiley & Sons, 1999.
- [40] Y. Polyanskiy and Y. Wu, *Information Theory: From Coding to Learning*. Cambridge University Press, 2022+ (book draft).